Published in final edited form as:

Mamm Genome. 2017 December ; 28(11-12): 487–497. doi:10.1007/s00335-017-9719-2.

Congenic Mice Demonstrate The Presence of QTLs Conferring Obesity and Hypercholesterolemia on Chromosome 1 in the TALLYHO Mouse

Jacaline K. Parkman[1], **James Denvir**[1], **Xia Mao**[1], **Kristy D. Dillon**[1], **Sofia Romero**[1], **Arnold M. Saxton**[2], and **Jung Han Kim**[1]

[1]Department of Biomedical Sciences, Joan C. Edwards School of Medicine, Marshall University, Huntington, WV 25755, USA

[2]Department of Animal Science, University of Tennessee, Knoxville, TN 37996, USA

Abstract

The TALLYHO (TH) mouse presents a metabolic syndrome of obesity, type 2 diabetes, and hyperlipidemia. Highly significant quantitative trait loci (QTLs) linked to adiposity (proximal) and hypercholesterolemia (distal) were previously identified on chromosome (Chr) 1 in a genome-wide scan of F2 mice from C57BL/6J (B6)×TH. In this study we generated congenic mouse strains that carry the Chr 1 QTLs derived from TH on a B6 background; B6.TH-Chr1-128Mb (128 Mb in size) and B6.TH-Chr1-92Mb (92 Mb in size, proximally overlapping). We characterized these congenic mice on chow and high fat (HF) diets. On chow, B6.TH-Chr1-128Mb congenic mice exhibited a slightly larger body fat mass compared with B6.TH-Chr1-92Mb congenic and B6 mice, while body fat mass between B6.TH-Chr1-92Mb congenic and B6 mice was comparable. Plasma total cholesterol levels were significantly higher in B6.TH-Chr1-128Mb congenics compared to B6.TH-Chr1-92Mb congenic and B6 mice. Again, there was no difference in plasma total cholesterol levels between B6.TH-Chr1-92Mb congenic and B6 mice. All animals gained more body fat and exhibited higher plasma total cholesterol levels when fed HF diets than fed chow, but these increases were greater in B6.TH-Chr1-128Mb congenics than in B6.TH-Chr1-92Mb congenic and B6 mice. These results confirmed the effect of the 128Mb TH segment from Chr 1 on body fat and plasma cholesterol values and showed that the distal segment of Chr 1 from TH is necessary to cause both phenotypes. Through bioinformatic approaches we generated a list of potential candidate genes within the distal region of Chr 1 and tested *Ifi202b* and *Apoa2*. We conclude that Chr 1 QTLs largely confer obesity and hypercholesterolemia in TH mice and can be promising targets for identifying susceptibility genes. Congenic mouse strains will be a valuable resource for gene identification.

Keywords

Obesity; Hypercholesterolemia; QTL; Congenic Mice; TALLYHO

Corresponding author: Jung Han Kim, PhD, Department of Biomedical Sciences, Joan C. Edwards School of Medicine, Marshall University, 1700 3rd Ave. #435K BBSC, Huntington, WV 25755, Tel: 304-696-3873, Fax: 304-696-7391, kimj@marshall.edu.

Conflicts of interest

The authors declare no conflict of interest.

Introduction

Obesity is associated with many comorbidities such as type 2 diabetes and coronary heart disease and affects 13% of the adult population worldwide, making it a major global health concern (Flynt and Daepp 2015). Hyperlipidemia characterized by increased plasma lipids, namely cholesterol and triglyceride, also signifies an increased risk of cardiovascular disease and often coexists with obesity (Erion and Corkey 2017). An important component in the development of obesity (Yazdi et al. 2015; Loos and Janssens 2017) and hyperlipidemia (Dron and Hegele 2016) is genetic factors. Although there are rare monogenic forms of obesity and hyperlipidemia, the genetic susceptibility to common forms is polygenic (Loos and Janssens 2017; Dron and Hegele 2016). Environmental factors are also a critical component in the development of obesity and hyperlipidemia, which is more likely the result of interplay between genes and environments with varying contributions in each individual (Doo and Kim 2015; Marais 2013). Among many environmental factors, nutrition is a strong connection between these interplays and especially, consuming food high in fat content is well known to promote obesity and hyperlipidemia (Doo and Kim 2015; Marais 2013).

The TALLYHO/Jng (TH) mouse is a polygenic model for human obesity and type 2 diabetes and characterized by increased adiposity, insulin resistance, hyperglycemia, and hyperlipidemia (Kim et al. 2001). In previous mapping study using F2 progeny of C57BL/6 (B6) and TH mice, we have identified two major quantitative trait loci (QTLs) on chromosome (Chr) 1; one linked to increased fat pad weight near *D1Mit215* and the other linked to hypercholesterolemia near *D1Mit113* (Stewart et al. 2010). Later, we named these QTLs; *Tabw3* for the adiposity peak and *Tachol1* for the hypercholesterolemia peak (Kim and Saxton 2012). To confirm the QTLs and develop a strategy for positional cloning of the responsible gene(s), in the present study, we generated and characterized congenic mice carrying these QTLs derived from the TH strain on a B6 genetic background.

Materials and Methods

Animals and diets

B6 mice were purchased from The Jackson Laboratory (Bar Harbor, ME) and maintained in our animal facility and TH mice used for construction of congenic strain were from our breeding colony. All mice had free access to food and water in a temperature and humidity controlled room with a 12-h light/dark cycle. At 4 weeks of age, mice were weaned onto standard rodent chow (14% kcal from fat, Purina 5001, PMI Nutrition, Brentwood, MO) or high fat (HF) diets (32% kcal from fat, 12266B, Research Diets; New Brunswick, NJ) and stayed on these diets throughout the study. Mice were euthanized by CO_2 asphyxiation, and blood was collected by cardiac puncture and plasma obtained by centrifugation (1,200 *g*) at 4°C and stored at −20°C. Tissues were collected, frozen in liquid nitrogen and stored at −80°C. All animal studies were carried out with the approval of Marshall University Animal Care and Use Committee.

Construction of congenic mice

Mice congenic for the Chr 1 QTL genomic region were generated by marker-assisted backcrossing (Kim et al. 2005). Briefly, B6 female and TH male mice were crossed to yield F1 and then F1 was backcrossed with B6. The progeny were then genotyped with single sequence length polymorphism (SSLP) markers to select heterozygotes for the QTL. Selected heterozygotes were backcrossed again with B6 mice. This procedure was repeated 10 times, at which point female and male heterozygotes were crossed to obtain offspring homozygous for TH alleles. Homozygous mice were then interbred to maintain congenic lines. The congenic segment stretched from *D1Mit213* to *D1Mit113*.

Genotyping by PCR

Genomic DNA was isolated from tail tips of mice using Gentra Puregene Mouse Tail Kit (Qiagen, Valencia, CA) for genotyping. SSLP primers synthesized (Sigma, St. Louis, MO) based on sequences from Mouse Genome Informatics (http://informatics.jax.org/) were assayed after PCR of genomic DNA by 3% agarose (Amresco, Solon, OH) gel electrophoresis and visualized with ethidium bromide (Thermo Fisher Scientific, Marietta, OH) staining.

Body composition

Quantitative magnetic resonance imaging was used to assess body composition including fat mass and lean mass in mice using EchoMRI-100 whole body composition analyzer (Echo Medical Systems, Houston, TX). A median of quintuple measurements for each animal was used (Parkman et al. 2016).

Indirect calorimetry, locomotor activity, and intake of food and water

An eight-chamber Comprehensive Laboratory Animal Monitoring System (CLAMS) (Columbus Instruments, Columbus, OH) was used to measure heat production, respiratory exchange ratio (RER), food intake, water intake, and locomotor activity (Stewart et al. 2012). All mice were acclimatized to monitoring cages for 24 hours prior to an additional 48 hours of recordings under the regular 12-hour light-dark cycle. In this system, heat production (kcal/hr) is calculated by multiplying the calorific value [CV = 3.815 + (1.232 × RER)] by the observed VO_2 (Heat = CV × VO_2). Heat production was then normalized by body weight to calculate energy expenditure (kcal/kg/hr) (Tschöp et al. 2011). RER is the ratio between the VCO_2 and VO_2 (RER = VCO_2/VO_2). Locomotor activity was determined a s ambulatory count, the number of times different infrared beams were broken in either the x- or y-axes during an interval.

Intraperitoneal glucose tolerance test

Mice were fasted overnight and injected with glucose in saline intraperitoneally (1mg/g body weight). Blood was collected via submandibular bleeding at 0, 15, 30, 60 and 120 minute after the injection. Blood glucose levels were measured and calculated using a One Touch Ultra2 Blood Glucose Monitoring System (Diagnostics Direct, Cape May Court House, NJ).

Non-fasting plasma insulin, triglyceride, and total cholesterol levels

Plasma insulin levels were determined using an ELISA kit (Crystal Chem, Downers Grove, IL). Plasma levels of total cholesterol (Thermo Electron, Louisville, CO) and free and total glycerol (Sigma) were determined using commercial colorimetric assays. Plasma true triglyceride concentrations were estimated by subtraction of free glycerol from total glycerol.

RNA isolation and real-time quantitative PCR (qRT-PCR)

Total RNA was isolated from epididymal adipose tissue and liver using RNeasy Plus Universal Midi Kit and RNeasy Midi Kit, respectively, according to the manufacturer's instructions (Qiagen). Total RNA (2 μg) was reverse-transcribed with SUPERSCRIPT RT using oligo dT as primer to synthesize first-strand cDNA in 20-μl volume according to manufacturer's instructions (Invitrogen, Waltham, MA). The primers used for the qRT-PCR for the interferon activated gene 202B (*Ifi202b*) gene were synthesized (Sigma) using sequences obtained from the published literature (forward: 5′-GGCAATGTCCAACCGTAACT-3′ and reverse: 5′-TAGGTCCAGGAGAGGCTTGA-3′) (Kimura et al. 2014) and the primers for apolipoprotein A135 II (*Apoa2*) gene were proprietary (PPM05347B, Qiagen). The real-time PCR reaction was carried out in a 25-μl volume in 1x SYBR Green PCR core reagents (Qiagen) containing 1 μl cDNA template diluate (1:5, v/v) and 6 pmol primers using the StepOne™ Real-Time PCR system (Thermo Fisher Scientific). For each sample, duplicate amplifications were performed and the average measurements used for data analysis. The *36B4* gene was used as a control to calculate the difference in average threshold cycle (ΔCt) values (Stewart et al. 2010).

RT-PCR and sequencing of the *Ifi202b* gene

The diluate cDNA described above was PCR amplified for $Ifi202b^{NZO}$ exon 1 and part of exon 2 using the Expand Long Template PCR system (Roche, Indianapolis, IN). The specific primers were forward (5′-CCCTCT TCCTTTACACCCAAC-3′) and reverse (5′-GCCTGGGACAGATGTCTC TT-3′) derived from Mus Musculus *Ifi202b* gene mRNA sequences (GenBank: JX945582.1) (Vogel et al. 2013). The PCR products were directly sequenced with primers originally used to amplify the PCR products. Sequencing was carried out automatically with fluorescent tags (Marshall University Genomics Core Facility).

Statistical analysis

Physiological data analysis—Variables were analyzed with analysis of variance, using a fixed effects factorial model of strain and diet and interaction. Least squares means were compared using Fisher's protected LSD at a 5% significance level.

Real-time qRT-PCR data analysis—Duplicate threshold cycle times were averaged for each mouse, and differences tested using a two-way ANOVA in SAS software (Cary, NC, USA), with an interaction contrast (housekeeping vs. gene interaction with strain or diet) used to estimate ΔΔCt. Data are presented as relative fold-change (Livak et al. 2001).

Bioinformatic analysis

We used a previously published catalog of sequence variants in the TH mouse (relative to the B6 strain) (Denvir et al. 2016) to list all variants lying between the markers *D1Mit498* (position 135,687,493 bp on Chr 1 in the GRCm38 genome build) and *D1Mit361* (186,261,999 bp on Chr 1). We restricted these to variants with the potential to alter the protein sequence: namely those with sequence ontology terms “frameshift_variant”, “inframe_deletion”, “inframe_insertion”, “missense_variant”, “stop_gained”, “stop_lost”, “initiator_codon_variant”, “splice_region_variant”, “splice_acceptor_variant”, or “splice_donor_variant”. We extracted molecular function and biological process terms for the genes containing each of these variants from the Gene Ontology (GO) database (Ashburner et al. 2000; The Gene Ontology Consortium 2015). We further restricted this collection of genes to contain only those that were associated to GO terms containing any of “cholesterol”, “fat”, “lipid”, “lipoprotein”, “lipase”, “glucose”, or “metabolic process”, to obtain a list of potential susceptibility genes.

Results

Generation of congenic mice for the obesity and hypercholesterolemia QTLs

In previous mapping study, we have identified two major QTLs on Chr 1; one linked to fat pad weight (*Tabw3*) near *D1Mit215* and the other linked to plasma cholesterol levels (*Tachol1*) near *D1Mit113* (Stewart et al. 2010; Kim and Saxton 2012). We established a congenic line by introgressing a TH-derived genomic fragment containing both *Tabw3* and *Tachol1*, defined by the flanking markers *D1Mit213* and *D1Mit113* (minimum of 128 Mb in size), onto B6 background for 10 generations. After the 10^{th} backcross generation, the offspring were intercrossed to generate B6.TH-Chr1-128Mb congenic mice (Fig. 1). Using this congenic line we generated a second congenic line, B6.TH-Chr1-92Mb, carrying a smaller fragment of Chr 1 with only *Tabw3*, defined by the flanking markers *D1Mit213* and *D1Mit498* (minimum of 92 Mb in size) (Fig. 1).

Increased adiposity and plasma cholesterol levels in B6.TH-Chr1-128Mb, but not in B6.TH184 Chr1-92Mb, congenic mice

When animals were fed a standard rodent chow, B6.TH-Chr1-128Mb congenic mice exhibited a small increase in body fat mass compared with B6.TH-Chr1-92Mb congenic and B6 mice, while body fat mass between B6.TH-Chr1-92Mb congenic mice and B6 mice was comparable (Fig. 2A). When fed HF diets, all animals had more body fat than when fed chow, but the increase was greater in B6.TH-Chr1-128Mb congenic mice than either B6.TH-Chr1-92Mb congenic or B6 mice (Fig. 2A). Again, body fat mass between B6.TH-Chr1-92Mb congenic and B6 mice was comparable on HF diets (Fig. 2A). The increased adiposity in B6.TH-Chr1-128Mb congenic mice on HF diets was accompanied by moderate increases in plasma insulin levels (Fig. 2B) and slightly impaired glucose tolerance during IPGTT (Fig. 2C), indicating some degree of insulin resistance.

Plasma total cholesterol levels were significantly higher in B6.TH-Chr1-128Mb congenic mice compared to B6.TH-Chr1-92Mb congenic and B6 mice on chow (Fig. 2D), confirming the presence of the *Tachol1* hypercholesterolemia QTL in the distal region of Chr 1. HF

diets induced an increase in total plasma cholesterol in all three groups compared to chow, with the greatest degree in B6.TH-Chr1-128Mb congenic mice (Fig. 2D). Plasma triglyceride levels were also significantly higher in B6.TH-Chr1-128Mb congenic mice compared to B6.TH-Chr1-92Mb congenic and B6 mice on chow (Fig. 2E). While HF diets induced an increase in plasma triglyceride levels in B6 mice, no increases were shown in both congenic mice.

These results confirmed the effect of the 128Mb TH segment from Chr 1 on body fat and plasma cholesterol values and showed that the distal segment of Chr 1 from TH is necessary to cause both phenotypes.

Energy expenditure, locomotor activity, and food and water intakes

We measured energy expenditure and intake and locomotor activity of B6, B6.TH-Chr1-128Mb and B6.TH-Chr1-92Mb mice on chow and HF diets by CLAMS and summarized in Table 1. Overall, with increased body mass the heat production (kcal/hr) per animal increased with HF diet feeding compared to chow. However, when the heat production was normalized to body weight (kcal/kg/hr), B6.TH-Chr1-128Mb congenic mice exhibited lower values than B6.TH-92Mb congenic and B6 mice on both chow and HF diets.

RER values were generally lower when animals were placed on HF diets compared to chow, demonstrating that whole body substrate metabolism was shifted towards fat oxidation. Additionally, compared to chow, in general animals consumed less food in grams on HF diets, balancing the total kcal intake. Water intake was also overall lower on HF diet. However, there was no genotype effect on RER, food intake, or water intake in either diet.

B6.TH-Chr1-128Mb congenic mice showed somewhat decreased locomotor activity compared to B6 and B6.TH-Chr1-92Mb mice on both diets, but it did not reach statistical significance.

The *Ifi202b* gene and *Apoa2* gene in B6.TH-Chr-128Mb congenic mice

The *Ifi202b* gene maps to the distal region of mouse Chr 1, near the *D1Mit113*, *Tachol1* QTL. It has been known that the gene expression levels of *Ifi202b* are closely associated with the obesity phenotype mediated by *Nob3* obesity QTL identified from F2 population of NZO and B6 strains; mRNA of *Ifi202b* was generated by the NZO allele but not by the B6 allele (Vogel et al. 2012). The B6 allele of *Ifi202b* contains a deletion that comprised exon 1 and the 5′-flanking region of *Ifi202b*, causing the lack of mRNA (Vogel et al. 2012; Vogel et al. 2017).

We performed PCR with primers corresponding to exon 1 and exon 2 of *Ifif202b* on the cDNA from adipose tissue in B6, congenic, and T H mice. B6.TH-Chr1-128Mb congenic and parental TH mice produced a PCR product, while B6 and B6.TH-Chr1-92Mb congenic mice did not as expected (Fig. 3A). We sequenced the PCR product of TH mice and found that they are the same as NZO except for one SNP in exon 1 (Fig. 3B). We then measured gene expression levels of *Ifi202b* in adipose tissue of B6 and congenic mice. Once the data were normalized to B6 mice having an expression value of one, B6.TH-Chr1-128Mb congenic mice had a relative expression value over 4 folds that of B6 mice, while B6.TH-

Chr1-92Mb congenic mice had a comparable value to that of B6 mice on chow (Fig. 3C). The gene expression of *Ifi202b* was significantly up-regulated in adipose tissue of B6.TH-Chr1-128Mb congenic mice when fed HF diets compared to chow (Fig. 3D).

The *Apoa2* gene is located near the *Tachol1.* An $Apoa2^b$ allele, characterized by Ala-to-Val substitution at amino acid residue 61, has been proposed to be hypermorphic in increasing plasma cholesterol levels in mice (Suto et al. 2004; Suto and Kojima 2017). The TH mouse carries the $Apoa2^b$ allele (Stewart et al. 2010 and Table 2). We examined the *Apoa2* gene expression in liver from B6 and B6.TH-Chr1-128Mb congenic mice. While the *Apoa2* gene expression levels were comparable between B6 and B6.TH-Chr1-128Mb congenic mice on chow, they were about 2-fold higher in B6.TH-Chr1-128Mb congenic than B6 mice on HF diets (Fig. 4).

Bioinformatic analysis of the distal region of Chr 1

We previously conducted a whole genome sequencing analysis for the TH mouse and generated a complete catalog of variants (relative to the B6 strain) (Denvir et al. 2016). We used this catalog to search potential candidates in the distal region of Chr 1. There were 167,833 SNPs and 36,284 indels in the region flanked by *D1Mit498* and *D1Mit361*; of these, 934 SNPs and 89 indels had the potential to directly alter the protein product. These variants occurred in 252 unique genes, of which 223 had molecular function or biological process terms associated with them in the GO database (supplementary table S1). This list of genes included *Apoa2* and *Ifi202b*. There were three missense variants in *Apoa2* and 11 missense variants in *Ifi202b* (Table 2).

We further filtered the list of 223 genes to include only those whose associated GO terms included “cholesterol”, “fat”, “lipase”, “lipoprotein”, “metabolic process”, or “glucose”. This resulted in a list of 36 genes. These genes, the type of variant(s) that occur in them, and their relevant associated GO terms are shown in Table 3.

Discussion

In this study, we generated congenic mice for previously mapped Chr 1 QTLs linked to adiposity (*Tabw3*) and hypercholesterolemia (*Tachol1*) derived from a TH fragment on a B6 background. On the B6 background, the TH derived Chr1 128Mb segment, containing the *Tabw3* and *Tachol1* QTLs, produced obesity and hypercholesterolemia in B6.TH-Chr1-128Mb congenic mice. However, contrary to our expectations, B6.TH-Chr1-92Mb congenic mice capturing the proximal segment corresponding with the *Tabw3* QTL failed to develop obesity. This may suggest that the effect of *Tabw3* alone may not be large enough or it may require interacting with other loci in the distal segment, potentially *Tachol1* or other obesity QTLs undetected from our original genome-wide study (Stewart et al. 2010). In this context, the obesity in B6.TH-Chr1-128Mb congenic mice may reflect this complexity. Generating congenic mice containing only the distal segment of Chr 1 may allow us to test this complexity.

Daily food intake of B6.TH-Chr1-128Mb congenic mice was comparable with that of B6 mice on both chow and HF diets, suggesting greater energy storage efficiency in the

congenic mice than B6. Energy expenditure determined by heat production normalized with body weight (kcal/kg/hr) was lower in B6.TH-Chr1-128Mb congenic mice than B6 mice. These findings are consistent with the characterization of parental TH strain (Parkman et al. 2016).

Based on the published knowledge, we tested *Ifi202b* and *Apoa2* genes as potential candidate genes within the distal region of Chr 1. It has been reported that the gene expression levels of *Ifi202b* are positively associated with the development of obesity in mice (Vogel et al. 2012; Vogel et al. 2017). The *Ifi202b* (also called *p202*) is known to play a role in cell proliferation and differentiation including adipocyte differentiation (Li et al. 2014). The mRNA levels of *Ifi202b* were significantly higher in adipose tissue from B6.TH-Chr1-128Mb than B6 mice and they were significantly upregulated in response to HF diets, suggesting a potential gene-diet interaction.

Several studies have identified highly significant cholesterol QTLs in the *Tachol1* interval and proposed the *Apoa2* gene as a likely candidate (Machleder et al. 1997; Suto et al. 2004; Suto et al. 2017). APOA2, synthesized in liver, has an antagonist effect on cellular cholesterol efflux (Bandarian et al. 2012). Transgenic mice overexpressing *Apoa2* develop hypercholesterolemia (Warden et al. 1993), while knockout of the gene in mice reduces plasma cholesterol levels (Weng and Breslow 1996). Further, transgenic mice overexpressing *Apoa2* have larger fat mass than controls (Castellani et al. 2001). The TH mouse carries the APOA2-Val61 allele that is putatively hypermorphic in increasing cholesterol levels. This polymorphism, however, does not seem to directly alter the mRNA levels of *Apoa2* as they were comparable between B6 and B6.TH-Chr1-128Mb congenic mice on chow. It was interesting to observe that the mRNA levels of *Apoa2* were significantly higher in B6.TH-Chr1-128Mb congenic than B6 mice on HF diets.

Through bioinformatic approaches using a catalog of sequence variants between B6 and TH mice we generated a list of potential candidate genes (Table 3). Among these, genes that cause obesity in knockout mice include the ATPase, Na^+/K^+ transporting, alpha 2 polypeptide (*Atp1a2*) gene (Kawakami et al. 2005) and poly (ADP-ribose) polymerase family, member 1 (*Parp1*) gene (Devalaraja-Narashimha and Padanilam 2010). On the other hand, transgenic mice overexpressing the upstream transcription factor 1 (*Usf1*) gene exhibit lower adiposity and lower plasma cholesterol levels than wild type mice (Wu et al. 2010).

In addition to the genes for which obesity or cholesterol phenotype was found in knockout or transgenic mice, other genes are also noticeable in the list based on known function. The hydroxysteroid (17-beta) dehydrogenase 7 (*Hsd17b7*) gene encodes an enzyme required for the cholesterol biosynthesis in liver and is known to be downregulated in a hypocholesterolemic rodent model (Nemoto et al. 2013). The phospholipase A2, group IVA (cytosolic, calcium-dependent) (*Pla2g4a*) gene encodes a calcium activated enzyme that catalyzes the hydrolysis of membrane phospholipids to release arachidonic acid, mediating eicosanoid-driven inflammation; polymorphism in *Pla2g4a* was associated with obesity resistant phenotype in a primate model (Harris et al. 2016). The C-reactive protein (*Crp*) gene and serum amyloid P-component (*Apcs,* also called *Sap*) gene are located in close proximity on Chr 1. CRP and SAP are a superfamily of proteins that are characterized by

pentraxin domain at the carboxyl-terminus and play key roles in innate immunity and inflammation (Garlanda et al. 2005). Human circulating CRP (Yudkin et al. 1997) and SAP (Jenny et al. 2007) concentrations were positively associated with BMI. Bochud et al. (2009) also suggested CRP as a causal factor for the obesity in human.

In conclusion, by analysis using congenic strains, we confirmed the effect of the 128Mb TH segment from Chr 1 in increasing body fat and plasma cholesterol values and demonstrated that the distal segment of Chr 1 from TH is necessary to cause both phenotypes. Our studies provided logical information regarding potential candidate genes for the Chr 1 QTL. The congenic strains will be a valuable resource for the identification of genes underlying these complex traits and their interactions with diets.

Supplementary Material

Refer to Web version on PubMed Central for supplementary material.

Acknowledgments

This work was supported in part by NIH/NIDDK Grant R01DK077202, American Heart Association Grant 0855300E, NIH/NIGMS P20GM103434 which funds the IDeA WV-INBRE program and supports the WV-INBRE Bioinformatics Core Facility, and institutional start-up funding from Marshall University to JHK.

References

Ashburner M, Ball CA, Blake JA, Botstein D, Butler H, Cherry JM, Davis AP, Dolinski K, Dwight SS, Eppig JT, Harris MA, Hill DP, Issel-Tarver L, Kasarskis A, Lewis S, Matese JC, Richardson JE, Ringwald M, Rubin GM, Sherlock G. Gene ontology: tool for the unification of biology. The Gene Ontology Consortium. Nat Genet. 2000; 25(1):25–29. [PubMed: 10802651]

Bandarian F, Daneshpour MS, Hedayati M, Naseri M, Azizi F. Identification of Sequence Variation in the Apolipoprotein A2 Gene and Their Relationship with Serum High-Density Lipoprotein Cholesterol Levels. Iran Biomed J. 2016; 20(2):84–90. [PubMed: 26590203]

Bochud M, Marquant F, Marques-Vidal PM, Vollenweider P, Beckmann JS, Mooser V, Paccaud F, Rousson V. Association between C-reactive protein and adiposity in women. J Clin Endocrinol Metab. 2009; 94(10):3969–3977. [PubMed: 19584180]

Castellani LW, Goto AM, Lusis AJ. Studies with apolipoprotein A-II transgenic mice indicate a role for HDLs in adiposity and insulin resistance. Diabetes. 2001; 50:643–651. [PubMed: 11246886]

Devalaraja-Narashimha K, Padanilam BJ. PARP1 deficiency exacerbates diet-induced obesity in mice. J Endocrinol. 2010; 205(3):243–252. [PubMed: 20338998]

Denvir J, Boskovic G, Fan J, Primerano DA, Parkman JK, Kim JH. Whole genome sequence analysis of the TALLYHO/Jng mouse. BMC Genomics. 2016; 17(1):907. [PubMed: 27835940]

Doo M, Kim Y. Obesity: interactions of genome and nutrients intake. Prev Nutr Food Sci. 2015; 20(1): 1–7. [PubMed: 25866743]

Dron JS, Hegele RA. Genetics of Lipid and Lipoprotein Disorders and Traits. Curr Genet Med Rep. 2016; 4(3):130–141. [PubMed: 28286704]

Erion KA, Corkey BE. Hyperinsulinemia: a Cause of Obesity? Curr Obes Rep. 2017; 6(2):178–186. [PubMed: 28466412]

Flynt A, Daepp MIG. Diet-related chronic disease in the northeastern United States: a model-based clustering approach. Int J Health Geogr. 2015; 14:25. [PubMed: 26338084]

Garlanda C, Bottazzi B, Bastone A, Mantovani A. Pentraxins at the crossroads between innate immunity, inflammation, matrix deposition, and female fertility. Annu Rev Immunol. 2005; 23:337–366. [PubMed: 15771574]

Gene Ontology Consortium. Gene Ontology Consortium: going forward. Nucleic Acids Res. 2015; 43(Database issue):D1049–D1056. [PubMed: 25428369]

Harris RA, Alcott CE, Sullivan EL, Takahashi D, McCurdy CE, Comstock S, Baquero K, Blundell P, Frias AE, Kahr M, Suter M, Wesolowski S, Friedman JE, Grove KL, Aagaard KM. Genomic Variants Associated with Resistance to High Fat Diet Induced Obesity in a Primate Model. Sci Rep. 2016; 6:36123. [PubMed: 27811965]

Kimura J, Ichii O, Nakamura T, Horino T, Otsuka S, Kon Y. BXSB-type genome causes murine autoimmune glomerulonephritis: pathological correlationbetwee n telomeric region of chromosome 1 and Yaa. Genes Immun. 2014; 15(3):182–189. [PubMed: 24477164]

Jenny NS, Arnold AM, Kuller LH, Tracy RP, Psaty BM. Serum amyloid P and cardiovascular disease in older men and women: results from the Cardiovascular Health Study. Arterioscler Thromb Vasc Biol. 2007; 27(2):352–358. [PubMed: 17138933]

Kawakami K, Onaka T, Iwase M, Homma I, Ikeda K. Hyperphagia and obesity in Na,K-ATPase alpha2 subunit-defective mice. Obes Res. 2005; 13(10):1661–1671. [PubMed: 16286513]

Kim JH, Sen S, Avery CS, Simpson E, Chandler P, Nishina PM, Churchill GA, Naggert JK. Genetic analysis of a new mouse model for non-insulin-dependent diabetes. Genomics. 2001; 74(3):273–286. [PubMed: 11414755]

Kim JH, Stewart TP, Zhang W, Kim HY, Nishina PM, Naggert JK. Type 2 diabetes mouse model TallyHo carries an obesity gene on chromosome 6 that exaggerates dietary obesity. Physiol Genomics. 2005; 22(2):171–181. [PubMed: 15870394]

Kim JH, Saxton AM. The TALLYHO mouse as a model of human type 2 diabetes. Methods Mol Biol. 2012; 933:75–87. [PubMed: 22893402]

Li H, Liu F, Guo H, Zhu Z, Jiao Y. Role of interferon-inducible protein 202 (p202) in the regulation of adipogenesis in mouse adipose-derived stem cells. Mol Cell Endocrinol. 2014; 382(2):814–24. [PubMed: 24246779]

Livak KJ, Schmittgen TD. Analysis of relative gene expression data using real-time quantitative PCR and the 2(-Delta Delta C(T)) Method. Methods. 2001; 25:402–408. [PubMed: 11846609]

Loos RJ, Janssens AC. Predicting Polygenic Obesity Using Genetic Information. Cell Metab. 2017; 25(3):535–543. [PubMed: 28273476]

Machleder D, Ivandic B, Welch C, Castellani L, Reue K, Lusis AJ. Complex genetic control of HDL levels in mice in response to an atherogenic diet. Coordinate regulation of HDL levels and bile acid metabolism. J Clin Invest. 1997; 99(6):1406–1419. [PubMed: 9077551]

Marais AD. Dietary lipid modification for mild and severe dyslipidaemias. Proc Nutr Soc. 2013; 72(3): 337–341. [PubMed: 23680392]

Nemoto K, Ikeda A, Ito S, Miyata M, Yoshida C, Degawa M. Comparison of constitutive gene expression levels of hepatic cholesterol biosynthetic enzymes between Wistar-Kyoto and stroke-prone spontaneously hypertensive rats. Biol Pharm Bull. 2013; 36(7):1216–1220. [PubMed: 23585482]

Parkman JK, Mao X, Dillon K, Gudivada A, Moustaid-Moussa N, Saxton AM, Kim JH. Genotype-dependent Metabolic Responses to Semi-Purified High-Sucrose High-Fat Diets in the TALLYHO/Jng vs. C57BL/6 Mouse during the Development of Obesity and Type 2 Diabetes. Exp Clin Endocrinol Diabetes. 2016; 124(10):622–629. [PubMed: 27437918]

Stewart TP, Kim HY, Saxton AM, Kim JH. Genetic and genomic analysis of hyperlipidemia, obesity and diabetes using (C57BL/6J × TALLYHO/JngJ) F2 mice. BMC Genomics. 2010; 11:713. [PubMed: 21167066]

Stewart TP, Mao X, Aqqad MN, Uffort D, Dillon KD, Saxton AM, Kim JH. Subcongenic analysis of tabw2 obesity QTL on mouse chromosome 6. BMC Genet. 2012; 13:81. [PubMed: 23025571]

Suto J, Takahashi Y, Sekikawa K. Quantitative trait locus analysis of plasma cholesterol and triglyceride levels in C57BL/6J × RR F2 mice. Biochem Genet. 2004; 42(9–10):324–363.

Suto JI, Kojima M. Identification of Quantitative Trait Loci That Determine Plasma Total-Cholesterol and Triglyceride Concentrations in DDD/Sgn and C57BL/6J Inbred Mice. Cholesterol. 2017; 2017:3178204. [PubMed: 28642824]

Tschöp MH, Speakman JR, Arch JR, Auwerx J, Brüning JC, Chan L, Eckel RH, Farese RV Jr, Galgani JE, Hambly C, Herman MA, Horvath TL, Kahn BB, Kozma SC, Maratos-Flier E, Müller TD,

Münzberg H, Pfluger PT, Plum L, Reitman ML, Rahmouni K, Shulman GI, Thomas G, Kahn CR, Ravussin E. A guide to analysis of mouse energy metabolism. Nat Methods. 2011; 9(1):57–63. [PubMed: 22205519]

Vogel H, Scherneck S, Kanzleiter T, Benz V, Kluge R, Stadion M, Kryvych S, Blüher M, Klöting N, Joost HG, Schürmann A. Loss of function of Ifi202b by a microdeletion on chromosome 1 of C57BL/6J mice suppresses 11β-hydroxysteroid dehydrogenase type 1 expression and development of obesity. Hum Mol Genet. 2012; 21(17):3845–3857. [PubMed: 22692684]

Vogel H, Montag D, Kanzleiter T, Jonas W, Matzke D, Scherneck S, Chadt A, Töle J, Kluge R, Joost HG, Schürmann A. An interval of the obesity QTL Nob3.38 within a QTL hotspot on chromosome 1 modulates behavioral phenotypes. PLoS One. 2013; 8(1):e53025. [PubMed: 23308133]

Vogel H, Jähnert M, Stadion M, Matzke D, Scherneck S, Schürmann A. A vast genomic deletion in the C56BL/6 genome affects different genes within the Ifi200 cluster on chromosome 1 and mediates obesity and insulin resistance. BMC Genomics. 2017; 18(1):172. [PubMed: 28201990]

Warden CH, Hedrick CC, Qiao JH, Castellani LW, Lusis AJ. Atherosclerosis in transgenic mice overexpressing apolipoprotein A-II. Science. 1993; 261:469–472. [PubMed: 8332912]

Weng W, Breslow JL. Dramatically decreased high density lipoprotein cholesterol, increased remnant clearance, and insulin hypersensitivity in apolipoprotein A-II knockout mice suggest a complex role for apolipoprotein A-II in atherosclerosis susceptibility. Proc Natl Acad Sci U S A. 1996; 93(25):14788–14794. [PubMed: 8962133]

Wu S, Mar-Heyming R, Dugum EZ, Kolaitis NA, Qi H, Pajukanta P, Castellani LW, Lusis AJ, Drake TA. Upstream transcription factor 1 influences plasma lipid and metabolic traits in mice. Hum Mol Genet. 2010; 19(4):597–608. [PubMed: 19995791]

Yazdi FT, Clee SM, Meyre D. Obesity genetics in mouse and human: back and forth, and back again. PeerJ. 2015; 3:e856. [PubMed: 25825681]

Yudkin JS, Stehouwer CD, Emeis JJ, Coppack SW. C-reactive protein in healthy subjects: associations with obesity, insulin resistance, and endothelial dysfunction: a potential role for cytokines originating from adipose tissue? Arterioscler Thromb Vasc Biol. 1999; 19(4):972–978. [PubMed: 10195925]

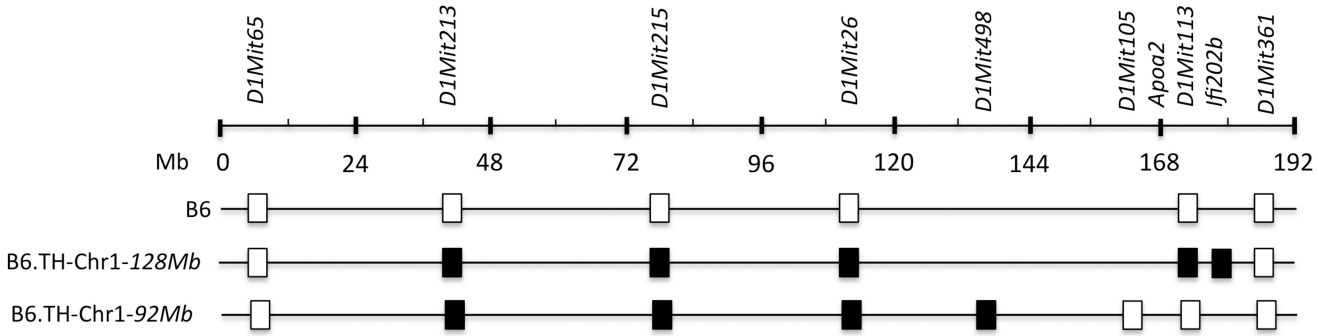

Figure 1.

B6.TH-Chr1 congenic intervals on chromosome 1. Genetic markers shown at the top were used to allelotype the congenic interval. The open and filled boxes represent a C57BL/6 (B6) and TALLYHO (TH) allele, respectively. Mb: Megabase

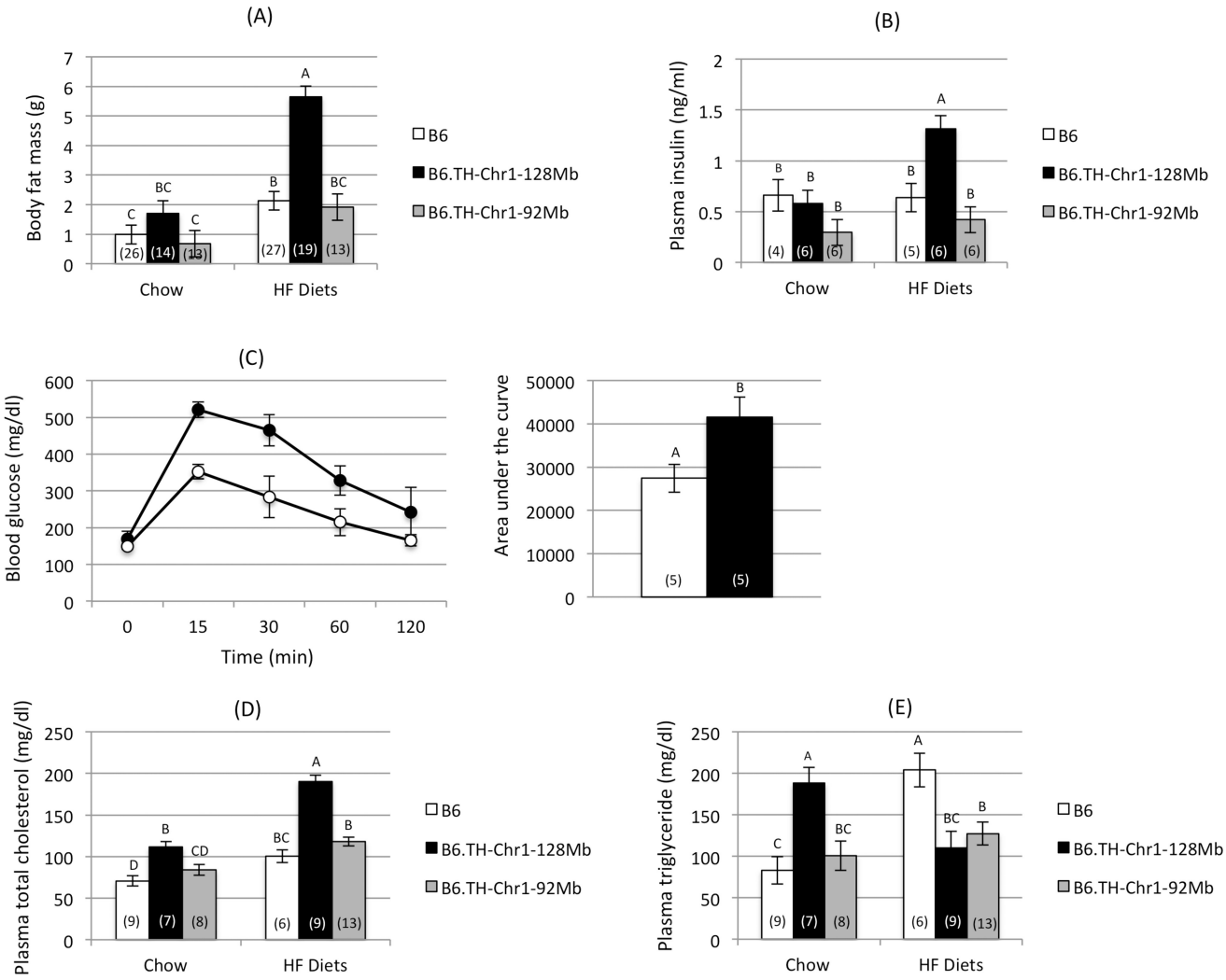

Figure 2.

(A) Body fat mass (14 wk), (B) plasma insulin levels (14–25 wk), (C) intraperitoneal glucose tolerance test (14–18 wk), and plasma (D) total cholesterol and (E) triglyceride levels (20–27 wk) in B6, B6.TH-Chr1-128Mb congenic, and B6.TH-Chr1-92Mb congenic mice fed chow and high fat (HF) diets (males). Data were reported as means ± SEM (N is indicated in each bar). Group means labeled with different letters are significantly different (P <0.05). wk: weeks of age

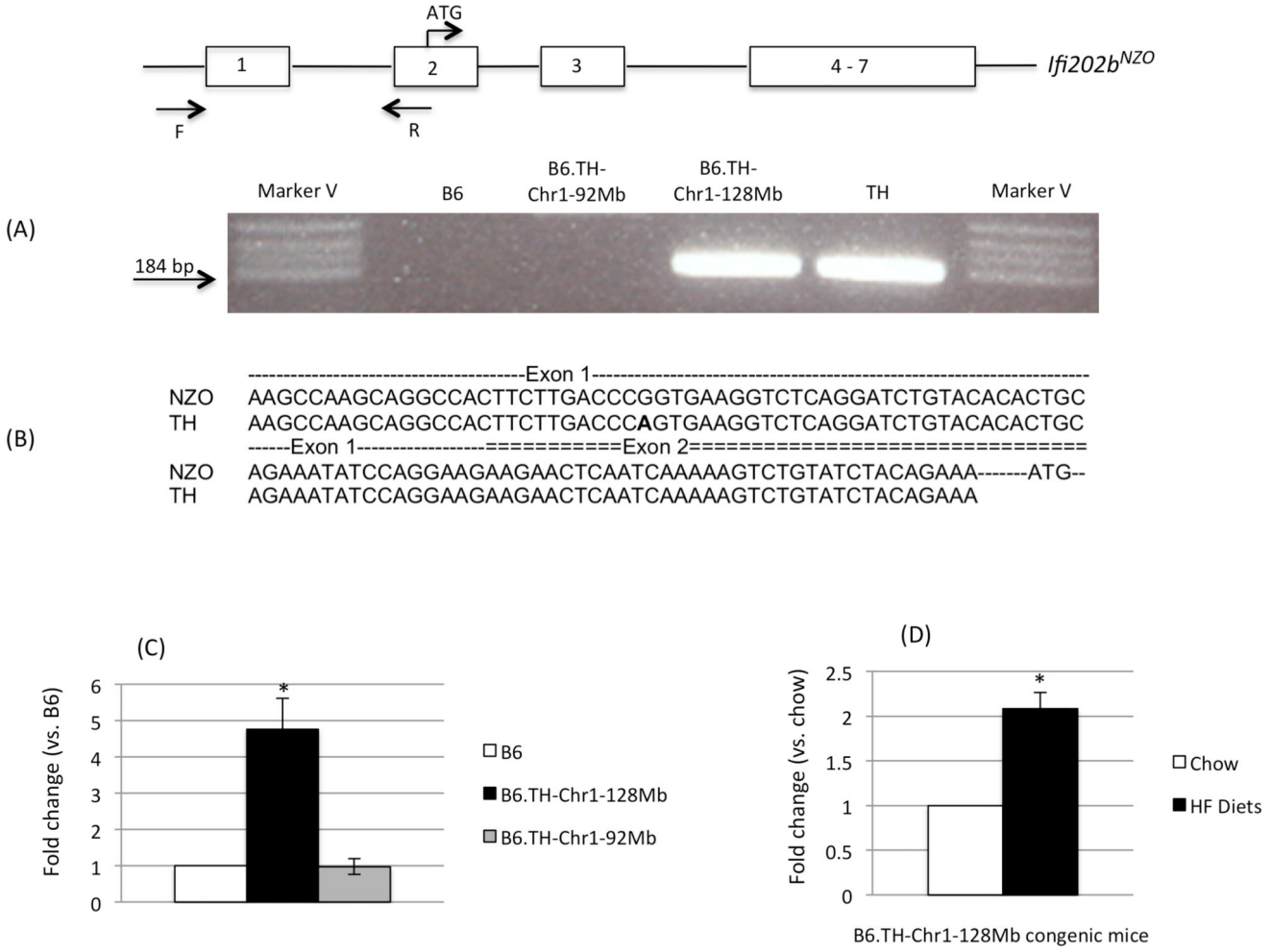

Figure 3.

Expression of *Ifi202b* in B6 and B6.TH-Chr1 congenic mice. (A) PCR amplification of exon 1 and part of exon 2 from cDNA (epididymal adipose tissue) of B6, B6.TH-Chr1-92Mb, B6.TH-Chr1-128Mb, and TH mice using a primer set of F and R as indicated in the scheme, (B) sequence comparison of the PCR product of TH to the sequence of NZO derived from GenBank accession number JX945582, and the mRNA levels of *Ifi202b* in epididymal adipose tissue from (C) B6, B6.TH-Chr1-128Mb, B6.TH-Chr1-92Mb mice on chow and (D) from B6.TH-Chr1-128Mb congenic mice on chow and HF diets. Data were reported as means ± SEM (N=3–4 each group, 17–27 weeks of age). * P <0.05.

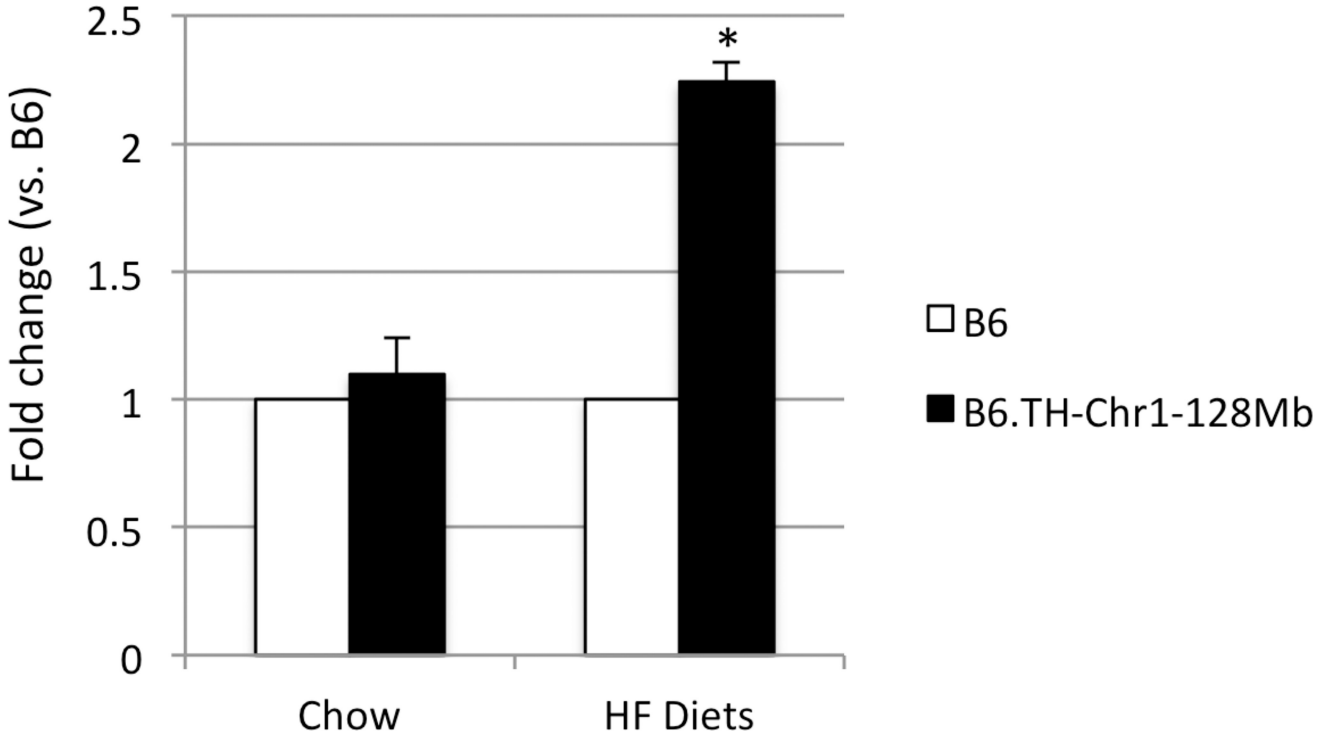

Figure 4.

The mRNA levels of *Apoa2* in liver from B6 and B6.TH-Chr1-128Mb congenic mice on chow and HF diets (males, 15–24 weeks of age). Changes in gene expression were expressed as fold change relative to mean values for B6 mice. Data were reported as means ± SEM (N=5–7 each group). * $P < 0.05$.

Table 1

Energy expenditure (heat production), respiratory exchange rate (RER), locomotor activity (ambulatory count), and food and water intakes in B6, B6.TH-Chr-128Mb congenic and B6.TH-Chr1-92Mb congenic mice on chow and HF diets over a 24-hour period (males, 19–23 weeks of age).

	Chow			HF diets		
	B6	**B6.TH-128Mb**	**B6.TH-92Mb**	**B6**	**B6.TH-128Mb**	**B6.TH-92Mb**
N	**17**	**15**	**9**	**7**	**4**	**13**
BW (g)	27.92 ± 0.57^{C}	30.73 ± 0.61^{B}	30.16 ± 0.79^{B}	32.43 ± 0.89^{B}	37.35 ± 1.18^{A}	30.95 ± 0.66^{B}
Heat						
kcal/hr	0.45 ± 0.01^{C}	0.44 ± 0.01^{C}	0.46 ± 0.01^{C}	0.56 ± 0.01^{A}	0.55 ± 0.01^{A}	0.51 ± 0.01^{B}
kcal/kg/hr	15.97 ± 0.26^{BC}	14.44 ± 0.28^{D}	15.37 ± 0.36^{C}	17.28 ± 0.41^{A}	14.82 ± 0.54^{CD}	16.68 ± 0.30^{AB}
RER	0.92 ± 0.01^{AB}	0.91 ± 0.01^{BC}	0.93 ± 0.01^{A}	0.89 ± 0.01^{CD}	0.87 ± 0.01^{D}	0.89 ± 0.01^{CD}
Food						
G	3.93 ± 0.15^{AB}	3.90 ± 0.16^{BC}	4.45 ± 0.21^{A}	3.33 ± 0.24^{CD}	3.17 ± 0.32^{D}	3.31 ± 0.18^{D}
kcal	13.20 ± 0.57^{A}	13.11 ± 0.60^{A}	14.95 ± 0.78^{A}	14.68 ± 0.89^{A}	13.98 ± 1.17^{A}	14.61 ± 0.65^{A}
Drink (ml)	3.54 ± 0.17^{A}	3.22 ± 0.18^{AB}	3.78 ± 0.23^{A}	2.72 ± 0.26^{BC}	2.40 ± 0.34^{C}	2.87 ± 0.19^{BC}
Ambulatory count	16210 ± 1106^{AB}	13623 ± 1178^{AB}	17395 ± 1520^{A}	16163 ± 1724^{AB}	11648 ± 2280^{B}	16284 ± 1265^{AB}

RER: respiratory exchange rate

ABCD means in a row with no common letter differ ($P<0.05$)

Table 2

Missense variants occurring in *Apoa2* and *Ifi202b*.

Nucleotide change (B6-TH)	Amino acid change (B6-TH)	Amino acid position
Apoa2		
T-A	D-E	43
A-G	M-V	49
C-T	A-V	61
Ifi202b		
A-C	S-A	432
T-A	T-S	379
A-G	L-P	350
A-T	F-I	292
T-C	K-E	204
G-A	T-I	187
T-A	I-F	142
A-C	I-M	141
T-A	I-F	127
T-C	E-G	109

Table 3

Genes in the region flanked by *D1Mit498* and *D1Mit361* with protein-altering variants that are associated with obesity-related Gene Ontology terms.

Gene	Variant type(s)	Go Terms
Abl2	missense_variant splice_donor_variant	positive regulation of phospholipase C activity
Acbd3	missense_variant	fatty-acyl-CoA binding; lipid metabolic process
Aldh9a1	splice_region_variant	metabolic process; carnitine metabolic process; cellular aldehyde metabolic process
Apcs	splice_region_variant	negative regulation by host of viral glycoprotein metabolic process; negative regulation of glycoprotein metabolic process
Apoa2	missense_variant	negative regulation of cholesterol import; high-density lipoprotein particle remodeling; cholesterol transporter activity; apolipoprotein receptor binding; high-density lipoprotein particle receptor binding; low-density lipoprotein particle remodeling; high-density lipoprotein particle clearance; negative regulation of cholesterol transport; cholesterol efflux; phospholipid efflux; phospholipid binding; fatty acid metabolic process; positive regulation of lipid catabolic process; phospholipid catabolic process; lipid transporter activity; triglyceride-rich lipoprotein particle remodeling; negative regulation of very-low-density lipoprotein particle remodeling; negative regulation of lipid catabolic process; lipoprotein metabolic process; cholesterol binding; lipid transport; cholesterol transport; positive regulation of cholesterol esterification; regulation of intestinal cholesterol absorption; reverse cholesterol transport; lipid binding; response to glucose; cholesterol metabolic process; negative regulation of lipase activity; high-density lipoprotein particle assembly; lipase inhibitor activity; high-density lipoprotein particle binding; negative regulation of cholesterol transporter activity; cholesterol homeostasis
Atp1a2	missense_variant splice_region_variant	ATP metabolic process
Bpnt1	missense_variant splice_region_variant	nucleobase-containing compound metabolic process
Crp	missense_variant	negative regulation of lipid storage; low-density lipoprotein particle receptor binding; regulation of low-density lipoprotein particle clearance; cholesterol binding; low-density lipoprotein particle binding
Ephx1	missense_variant splice_region_variant	cellular aromatic compound metabolic process
Eprs	missense_variant splice_region_variant	metabolic process
Exo1	splice_region_variant	nucleobase-containing compound metabolic process; DNA metabolic process
Fh1	missense_variant splice_region_variant	fumarate metabolic process; malate metabolic process
Hhipl2	missense_variant splice_acceptor_variant splice_region_variant	carbohydrate metabolic process
Hsd17b7	missense_variant	cholesterol biosynthetic process; lipid metabolic process
Itpkb	missense_variant splice_region_variant	inositol trisphosphate metabolic process

Gene	Variant type(s)	Go Terms
Kmo	intron_variant missense_variant splice_region_variant	NAD metabolic process; kynurenine metabolic process
Lamc1	missense_variant splice_region_variant	glycosphingolipid binding
Marc1	missense_variant splice_region_variant	nitrate metabolic process
Marc2	splice_region_variant	nitrate metabolic process
Mark1	missense_variant splice_region_variant	lipid binding
Mia3	inframe_insertion missense_variant splice_region_variant	lipoprotein transporter activity; lipoprotein transport
Ncf2	splice_region_variant	superoxide metabolic process; response to glucose
Ncstn	missense_variant	beta-amyloid metabolic process
Nit1	missense_variant splice_region_variant	nitrogen compound metabolic process
Npl	splice_region_variant	metabolic process; carbohydrate metabolic process
Parp1	splice_region_variant	mitochondrial DNA metabolic process; DNA metabolic process
Pex19	splice_region_variant	negative regulation of lipid binding
Pla2g4a	splice_region_variant	metabolic process; calcium-dependent phospholipase A2 activity; calcium-dependent phospholipid binding; phospholipase A2 activity; phospholipid catabolic process; lipid metabolic process; lysophospholipase activity; phospholipase activity; lipid catabolic process; arachidonic acid metabolicprocess
Ppox	splice_region_variant	protoporphyrinogen IX metabolic process
Psen2	missense_variant splice_region_variant	cellular protein metabolic process; beta-amyloid metabolic process
Rab3gap2	missense_variant splice_region_variant	positive regulation of protein lipidation
Rnasel	missense_variant splice_region_variant	fat cell differentiation; positive regulation of glucose import in response toinsulin stimulus
Soat1	missense_variant splice_region_variant	cholesterol O-acyltransferase activity; cholesterol efflux; cholesterol binding; cholesterol metabolic process; cholesterol storage; very-low-density lipoprotein particle assembly; lipid metabolic process; steroid metabolic process; cholesterol homeostasis; cholesterol esterification
Tnr	missense_variant	sphingolipid binding

Gene	Variant type(s)	Go Terms
Uap1	missense_variant splice_region_variant	metabolic process; UDP-N-acetylglucosamine metabolic process
Usf1	inframe_deletion	glucose metabolic process; positive regulation of transcription from RNA polymerase II promoter by glucose; lipid homeostasis